Distribution Agreement

In presenting this thesis as a partial fulfillment of the requirements for a degree from Emory University, I hereby grant to Emory University and its agents the non-exclusive license to archive, make accessible, and display my thesis in whole or in part in all forms of media, now or hereafter now, including display on the World Wide Web. I understand that I may select some access restrictions as part of the online submission of this thesis. I retain all ownership rights to the copyright of the thesis. I also retain the right to use in future works (such as articles or books) all or part of this thesis.

Genevieve Wilson 13 Apr 2021

The Role of the Neuropeptide Galanin in Locus Coeruleus Degeneration

by

Genevieve Wilson

Dr. David Weinshenker, PhD

Adviser

Neuroscience and Behavioral Biology

Dr. David Weinshenker, PhD

Adviser

Dr. Yoland Smith, PhD

Committee Member

Dr. Lary Walker, PhD

Committee Member

2021

The Role of the Neuropeptide Galanin in Locus Coeruleus Degeneration

By

Genevieve Wilson

Dr. David Weinshenker, PhD

Adviser

An abstract of

a thesis submitted to the Faculty of Emory College of Arts and Sciences

of Emory University in partial fulfillment

of the requirements of the degree of

Bachelor of Science with Honors

Neuroscience and Behavioral Biology

2021

Abstract

The Role of the Neuropeptide Galanin in Locus Coeruleus Degeneration

By Genevieve Wilson

The neuropeptide galanin, which is widely expressed in both the brain and periphery, appears to have both neuromodulatory and neurotrophic activity in the nervous system. In its neurotrophic role, galanin can convey a protective effect to neurons under some conditions, presenting a potential therapeutic target for various common neurodegenerative diseases such as Alzheimer's Disease (AD) and Parkinson's Disease (PD). The locus coeruleus (LC), the major noradrenergic nucleus in the brain, co-expresses galanin in about 80% of its neurons. The LC is one of the first regions to show signs of damage in neurodegenerative diseases such as AD, and galanin-containing LC neurons are relatively spared in AD compared to LC neurons that do not express galanin. Therefore, the goal of the present research was to further elucidate the potential neuroprotective role of galanin in response to LC damage. This work assessed whether genetic overexpression (Gal OX) or knockout ($Gal^{cKO\text{-}Dbh}$) of LC-derived galanin in mice altered the neurotoxicity induced by the LC-specific neurotoxin, DSP-4. DSP-4 was administered either acutely (1 injection) or chronically (5 injections over three months). LC neuron and fiber integrity were assessed in the LC and several of its forebrain targets using immunohistochemistry for the norepinephrine transporter (NET). Microglial activation was also assessed using immunohistochemistry for ionized calcium binding adaptor molecule 1 (IBA-1), a protein expressed in microglia which is upregulated during microglial activation. In general, chronic DSP-4 caused more damage to LC neurons than acute DSP-4, and the effects were similar between genotypes. However, there was a consistent trend for a greater reduction of NET immunoreactivity and a failure to increase IBA-1 in Gal^{cKODbh} mice following acute DSP-4 administration, suggesting that endogenous galanin protects LC neurons against neurotoxin-induced degeneration under certain conditions, potentially via a microglial mechanism. Future work should further elucidate the role of galanin in response to LC damage by exploring its relationship to microglial pro- and anti-inflammatory activity.

The Role of the Neuropeptide Galanin in Locus Coeruleus Degeneration

By

Genevieve Wilson

Dr. David Weinshenker, PhD

Adviser

A thesis submitted to the Faculty of Emory College of Arts and Sciences

of Emory University in partial fulfillment

of the requirements of the degree of

Bachelor of Science with Honors

Neuroscience and Behavioral Biology

2021

Acknowledgments

I would like to thank Dr. David Weinshenker for guiding me in the development of this project and supporting me throughout the process. I would also like to thank all of the Weinshenker lab members for their support, but especially Dr. Rachel Tillage for her mentorship and training.

I am also extremely grateful for the guidance and support provided to me by Dr. Yoland Smith and Dr. Lary Walker as part of my thesis committee. Their feedback has been invaluable.

Additionally, I would like thank Dr. Leah Roesch for her guidance throughout the research process.

Table of Contents

The Role of the Neuropeptide Galanin in Locus Coeruleus Degeneration

By Genevieve Wilson

Introduction

The locus coeruleus (LC) is a brainstem nucleus which is implicated in several neurodegenerative diseases. It is thought to be one of the first areas in which protein aggregates build up and cause neuronal dysfunction and death in the early stages of diseases such as Alzheimer's Disease (AD) and Parkinson's Disease (PD) (Braak and Del Tredici, 2012, 2013; Haglund et al., 2006). Furthermore, damage to the LC has been shown in animal models to exacerbate the disease process in connected brain regions via tau and amyloid beta (Jardanhazi-Kurutz, D. et al., 2010; Chalermpalanupap et al., 2018). While the LC is the brain's main source of norepinephrine (NE), it also produces other neuromodulators that have been much less widely studied (Sara, 2009). Galanin is one such neuropeptide co-expressed with NE in about 80% of LC neurons (Schwartz and Luo, 2015; Weinshenker, 2018). While previous studies have shown that galanin has a neuroprotective role in instances of damage to the nervous system, the role of galanin in protecting LC neurons from damage has not been explored in much depth. A better understanding of galanin's function in instances of LC damage could lead to improved understanding of neurodegenerative diseases in which the LC is a key structure. Moreover, galanin's neuroprotective capabilities may offer an avenue for future preventative therapies.

The Locus Coeruleus

Anatomy and Connectivity

The locus coeruleus (LC) is a small, tightly-packed bilateral nucleus in the rostral pons of the brainstem, caudal to the tectum of the midbrain. The so-called "blue spot," LC neurons are pigmented with neuromelanin made from norepinephrine (NE) metabolites, heavy metals, proteins, and lipids. Excluding the basal ganglia, the LC projects to most areas of the brain, including the amygdala, hypothalamus, cerebellum, spinal cord, cerebral cortex, and hippocampus (Figure 1) (Swanson and Hartman, 1975; Oleskevich, Descarries, and Lacaille, 1989). Information is consolidated in the LC, with inputs coming mainly from the medulla, prefrontal cortex, and hypothalamus (Schwartz et al, 2015). With widespread connections and the prevalence of NE in the brain, the LC plays a role in regulating many important processes such as memory, attention, arousal, stress responses, and mood (Aston-Jones and Cohen, 2005; Samuels and Szabadi, 2008; Sara, 2009).

Organization and Heterogeneity

Despite the fact that LC neurons all contain NE, these neurons are not identical in morphology, molecular composition, or downstream targets (Figure 2). Different cell morphologies have been observed in the LC, with larger multipolar cells in the ventral portion, smaller fusiform cells in the dorsal portion, and other cells interspersed throughout. LC neurons also vary in their molecular composition, with about 80% co-expressing galanin, located primarily in the dorsal and central portions of the LC. Neuropeptide Y (NPY) is also co-expressed in about 20% of LC

neurons, most of which are located in the dorsal portion of the LC. LC neurons also display differences in the distribution and prevalence of adrenoreceptors. In terms of organization of projection targets, it appears that the LC may be structured topographically. Studies have shown that the dorso-rostral part contains neurons projecting to the hippocampus and neocortex, while the caudo-ventral part contains neurons projecting to the cerebellum and spinal cord (Loughlin, Foote, and Grzanna, 1986; Schwartz and Luo, 2015).

LC Vulnerability

The LC is particularly vulnerable to damage for various reasons (Figure 3). Firstly, the production of NE is costly because it is highly reactive and releases metabolites such as dihydroxyphenylglycolaldehyde, which leads to the cleavage of tau into aggregation-prone forms. On top of this, individual neurons in the LC store toxic NE as metabolites and heavy metals as neuromelanin, which can cause neuroinflammation and neurodegeneration upon release (Oertel et al., 2019). Additionally, LC projections are widespread throughout the brain, as well as highly branched and poorly myelinated or unmyelinated. This results in high energy needs in order to broadly propagate rapid action potentials through thinly insulated axons. LC neurons also have autonomous pacemaker activity, meaning that they require high mitochondrial activity levels and are highly sensitive to mitochondrial damage. Because of its proximity to the fourth ventricle, the LC is also especially vulnerable to any toxins present in the cerebrospinal fluid, such as environmental toxins including heavy metals. It is postulated that these factors make the LC particularly vulnerable to damage, therefore making the LC one of

the first areas to experience pathology and degeneration in AD and PD (Janitzky, 2020; Matchett et al., 2021).

LC Neuron Loss in Disease

LC cell loss is a key feature of several neurodegenerative diseases, including both Parkinson's disease, Alzheimer's disease, and possibly multiple sclerosis (Braak and Del Tredici, 2012, 2013; Haglund et al., 2006). Accordingly, many of the functions that decline in these diseases are those that are regulated by the LC. It has also been shown that LC neuron loss, which is much greater than the loss of surrounding nuclei, is correlated with the duration of illness (Zarow et al., 2013). Studies in rodent models of AD have shown that LC damage or neuron loss occurs as part of the disease progression. On top of this, our lab and others have demonstrated that damage to the LC also accelerates AD pathology in other parts of the brain in rodent models of the disease (Chalermpalanupap et al., 2018; Heneka et al., 2006).

Because of the types of cognitive abilities that decline in AD and other neurodegenerative diseases, combined with the prevalence of NE in the brain, it is thought that NE loss has a major role in promoting disease symptoms (Trillo et al., 2013). Some studies have found that NE has a protective effect on cells by inducing an anti-inflammatory response. However, the other neuromodulators produced by the LC may play a role in disease progression, and therefore merit further exploration.

Norepinephrine

The neurotransmitter NE, the majority of which is produced by the LC, has many essential roles in the brain including for arousal, stress, and attention. NE is a catecholamine neurotransmitter produced in neurons from tyrosine using the enzymes tyrosine hydroxylase (TH), aromatic acid decarboxylase (AADC), and dopamine beta-hydroxylase (DBH). In this enzymatic pathway, DBH converts dopamine to NE, which is then stored in vesicles at the axon terminal in preparation for release into the synapse (Musacchio, 2013). In downstream targets of the LC, NE binds to α- and β-adrenoreceptors at the synapse as a primarily excitatory neurotransmitter, acting through Gq (α1-receptors) and Gs (β-receptors) coupled receptor cascades. NE is also released extra-synaptically from the soma/dendrites of LC neurons, acting locally to inhibit LC neuron firing and NE release by acting on the Gi-coupled α_2-adrenoreceptor. The α_2-adrenoreceptor causes the hyperpolarization and therefore inhibition of LC neurons (Bacon et al., 2020; Hongping, et al, 2012). While the majority of research on the LC has focused on NE, the other neuromodulators produced by the LC merit more exploration (Sara, 2009; Trillo et al., 2013). The neuropeptide galanin, for instance, is co-expressed with norepinephrine in 80% of LC neurons, and its contributions to the function of the LC have been largely unexplored (Weinshenker, 2018).

Galanin

Overview and Distribution

Galanin is a 29-amino acid neuropeptide tied to a variety of functions in the body, including anxiety, memory, nociception, and arousal. It is widely produced throughout the nervous system, though the majority is produced in the central nervous system and in the intestine by cells expressing the GAL gene (Lang et al., 2015; Wynick, Thompson, and McMahon, 2001). Collections of galanin-expressing neurons are found in the LC, area postrema, bed nucleus of the stria terminalis, and hypothalamic nuclei including the medial preoptic nucleus and paraventricular nucleus of the thalamus (Jacobowitz, Kresse, and Skofitsch, 2004) (Figure 3). Immunohistochemistry in the rat brain has also revealed the greatest galanin-positive fiber density in the LC, hippocampus, hypothalamus, and preoptic area, among other areas (Skofitsch and Jacobowitz, 1985). Galanin receptor density generally correlates with fiber density, especially in the hypothalamic area. The greatest density of receptors is found in the amygdala, though they are also scattered throughout the PNS (Jacobowitz, Kresse, and Skofitsch, 2004).

As a “classic” neuropeptide, galanin is stored in large, dense-core vesicles and is co-expressed in various types of neurons alongside their “defining” neurotransmitters. After a neuron has fired a rapid burst of action potentials, galanin is released into the synapse and also extrasynaptically from soma and dendrites (Lang et al., 2015).

Neuromodulatory Roles

At the synapse, galanin acts as a neuromodulator via three G-protein-linked receptors: GalR1, GalR2, and GalR3, which allow for galanin's broad range of actions in the body. GalR1 is Gi-coupled and is thought to act via cAMP/PKA inhibition and to function as a neuromodulator for nociception, anxiety, and reward, primarily in the CNS. GalR2 is thought to have similar effects by inhibiting adenylate cyclase, but it also has been found to couple to Gq and phospholipase C activation, which leads to an influx of Ca^{2+} and neurotransmitter release. It is thought to possess neurotrophic-like properties and regulates processes such as neural development, neural survival, and neurogenesis. GalR3 is the least well-understood galanin receptor subtype, though it is thought to primarily be located in the PNS and may combine some of the actions of GalR1 and GalR2 (Lang et al., 2015; Šípková et al., 2017; Webling et al., 2012). In the CNS, it appears that galanin inhibits both cholinergic and noradrenergic neurons. In the hippocampus, for instance, galanin has been shown to reduce cholinergic neuronal activity and therefore inhibit functions such as long-term potentiation, which is a critical process underlying learning and memory (Counts, Perez, and Mufson, 2010). Additionally, galanin acts on the LC to inhibit activity and thereby appears to serve as a feedback mechanism to regulate LC activity after bursts of firing (Ma et al., 2001).

Neurotrophic Roles

Throughout the nervous system, galanin is upregulated in response to injury. Elevated galanin levels have been identified in brain regions lesioned in rats and particularly in regions with amyloid-beta protein buildup (Gabriel, Knott, and Haroutunian, 1995; Diez et al., 2000). Galanin

also appears to be involved in the maintenance of dendritic spines and to promote outgrowths from hippocampal and dorsal root ganglion neurons (Hobson et al., 2008; Hobson et al., 2013). Furthermore, partial destruction of noradrenergic or LC cell bodies causes increased LC neuron activity (Chiodo et al., 1982; Szot et al., 2016). In AD-related LC damage, this leads to increased galanin and galanin receptor levels in downstream targets of the LC (Counts et al., 2003). Beal et al. (1990) reported that galanin levels appear to be twice as high in the brains of late-stage AD patients as in controls. Intriguingly, in the cholinergic nucleus basalis, it has been identified that galanin and galanin receptor levels appear to be highest where AD-related degeneration is lowest, and it has also been reported that galanin-expressing LC neurons are relatively spared in AD (Miller et al.,1999; Mufson et al., 2000).

While this evidence points to a primarily beneficial role of galanin, evidence has shown that galanin also inhibits cognition via perturbing several important processes such as long-term potentiation (Counts, Perez, and Mufson, 2008; Fisone et al., 1987). These effects would serve to exacerbate symptoms of neurodegenerative diseases such as AD. Because the role of galanin is likely multi-faceted and remains controversial, further work is needed to explore its mechanisms in the context of LC-specific damage.

Hypothesis and Expected Results

The overall goal of this study was to test the hypothesis that galanin can protect LC neurons from damage. We expect to find that wild type (WT) mice treated with a neurotoxin that causes LC-specific neurodegeneration will experience degeneration of LC cell bodies and LC projections

to the prefrontal cortex, hippocampus, and anterior insula. Additionally, we predict that WT mice will exhibit increased microglial activation representing an immune response. However, we anticipate that transgenic mice overexpressing galanin in noradrenergic neurons (Gal OX mice) will exhibit reduced degeneration compared to WT.

We also predict that conditional knockout mice lacking galanin in noradrenergic neurons ($Gal^{cKO\text{-}Dbh}$ mice) will be more vulnerable to the neurotoxic lesion and therefore exhibit greater degeneration. Such a result would provide further evidence for the neuroprotective effect of galanin and represent a potential mechanism for addressing the initial indications of neurodegenerative diseases which appear early on in the LC.

Materials and Methods

The experiments in this thesis were conducted at Emory University, and all protocols conform to the National Institutes of Health *Guide for the Care and Use of Laboratory Animals* and were approved by the Emory University Institutional Animal Care and Use Committee.

Subjects

Eighty-six mice were used in this study. Twenty mice were transgenic Gal OX mice that were generated with a transgene containing the mouse galanin gene driven by the human dopamine β-hydroxylase (DBH) promoter, resulting in overexpression of galanin in noradrenergic neurons

(Jackson Labs stock #004996), and 17 mice were WT littermate controls (Crawley et al., 2002). Sixteen of these mice were males, and 21 were females.

An additional 24 mice lacked galanin specifically in noradrenergic neurons ($Gal^{cKO\text{-}Dbh}$), and 25 were WT littermate controls. To create the line of $Gal^{cKO\text{-}Dbh}$ mice, we crossed mice with a conditional knockout allele of *Gal* (Gal^{cKO}) and mice with a knock-in of the cre driver allele controlled by noradrenergic-specific Dbh promoter (DBH^{cre}). Gal^{cKO} mice were generated using loxP-flanked *Gal* exon 3 and FRT-flanked LacZ and Neo cassettes in embryonic stem cells. Mice with the Gal^{cKO} allele have a *Gal* exon 3 that can be deleted by the enzyme Cre recombinase. DBH^{cre} mice were generated via insertion of rox-flanked transcriptional stop cassette, cre cDNA, rabbit β-globin polyadenylation cassette, and attB/attP-flanked neomycin resistance cassette into the Dbh locus immediately before the start codon in embryonic stem cells. Mice with the DBH^{cre} allele express Cre recombinase in noradrenergic neurons. Therefore, mice with both this allele and the conditional knockout allele of *Gal* have a deletion of Gal exon 3 and therefore no galanin expression in noradrenergic neurons (Tillage et al., 2020).

While weights varied slightly over time, each subject weighed between 20-35 grams on average. Mice were group-housed from birth, with no more than five animals per cage. Mice were maintained on a 12/12 h light-dark cycle with access to food and water *ad libitum*.

Neurotoxic Lesions

Mice were injected intraperitoneally (i.p.) with the neurotoxin N--N-ethyl-2-bromobenzylamine (DSP-4; Sigma-Aldrich, St. Louis, MO, catalog #C8417), which has been shown to selectively target and destroy axons and cell bodies of the LC (Ross and Stenfors, 2015). This served to simulate the degeneration of the LC observed in human AD. Literature indicates that a single DSP-4 treatment destroys LC axons and terminals while leaving cell bodies intact, mimicking early AD, while multiple DSP-4 injections result in cell death reminiscent of later-stage AD (Grzanna et al., 1989; Ross, 1976; Szot et al., 2010). Mice were between 3-8 months of age at the time of injection.

Mice were divided into four treatment groups for the Gal OX arm: WT + DSP-4 (50 mg/kg, i.p.), WT + saline, Gal OX + DSP-4 (50 mg/kg, i.p.), and Gal OX + saline, with sexes balanced across the groups. For the $Gal^{cKO\text{-}Dbh}$ arm, the four treatment groups were WT + DSP-4 (10 mg/kg, i.p.), WT + saline, $Gal^{cKO\text{-}Dbh}$ + DSP-4 (10 mg/kg, i.p.), and $Gal^{cKO\text{-}Dbh}$ + saline, with sexes balanced across the groups. The dosage was lowered in the $Gal^{cKO\text{-}Dbh}$ arm in order to prevent a predicted floor effect arising from the potentially heightened vulnerability to DSP-4 resulting from the absence of noradrenergic galanin (Figure 4).

In order to observe the effect of acute mild degeneration, 18 mice in the Gal OX arm and 26 mice in the $Gal^{cKO\text{-}Dbh}$ arm were injected once and sacrificed 1 week later (acute paradigm). To examine the effects of more chronic and severe degeneration, the remaining 19 mice in the Gal OX arm and the remaining 23 in the $Gal^{cKO\text{-}Dbh}$ arm received additional injections one week after the first, and then once per month for the following 4 months (chronic paradigm). One week

after their final injection, mice were sacrificed (Figure 5). This procedure was developed based on previous work in our lab using transgenic mouse models of AD and DSP-4 (Chalermpalanupap et al., 2018).

Perfusions and Tissue Collection

Prior to tissue collection, mice were anesthetized according to IACUC guidelines in a chamber with the inhalant anesthetic isoflurane. Following this, mice were transcardially perfused with cold 0.1M KPBS (saline), followed by 4% paraformaldehyde (PFA). Brains were removed and stored overnight at 4° C in 4% PFA, then transferred to a 30% sucrose solution for at least 48 hours prior to sectioning.

Immunohistochemistry

To ascertain the extent of LC axonal and cell body degeneration, we used immunohistochemistry for the NE transporter (NET), which is a validated marker for noradrenergic axons and cell bodies. Immunohistochemistry for ionized calcium-binding adaptor molecule 1 (IBA-1) was also performed to assess microglia. IBA-1 is upregulated during microglial activation, which is known to follow damage to the nervous system. NET fluorescent intensity was quantified in noradrenergic fibers in forebrain targets of the LC. IBA-1 was quantified in the same regions, which included the dentate gyrus (DG) of the dorsal hippocampus, anterior cingulate cortex (ACC) of the prefrontal cortex, and anterior insula (AI). NET and IBA-1 fluorescent intensities were also quantified in the LC, which contains the noradrenergic cell bodies.

To prepare brain sections for immunohistochemistry, brains were frozen and sliced with a cryostat into 40-micron-thick sections at -20°C. Sections were stored in cryoprotectant at -20°C until staining. First, sections were washed in 1x phosphate-buffered saline (PBS) for 5 min, and then incubated at room temperature for 1 h in a blocking solution of 0.1% PBS-Triton and 5% normal goat serum (NGS) to prevent nonspecific binding of proteins. Following this, the primary antibodies, mouse anti-NET and rabbit anti-IBA-1, were added, and tissue was incubated for 48 h at 4°C while rocking. Tissue was again washed in 1x PBS 3 times for 5 minutes each and then was incubated with secondary antibodies for 2 h at room temperature while rocking. Secondary antibodies were conjugated to a fluorochrome in order to allow for fluorescence microscopy: goat anti-mouse (488 nm) was used to label NET in green and goat anti-rabbit (568 nm) was used to label IBA-1 in red. After washing again, sections were mounted onto slides. The slides were coverslipped with Fluoromount mounting media containing the fluorescent nuclear stain DAPI (4',6-diamidino-2-phenylindole).

Image Scoring

For viewing and quantifying cellular elements in the sections, the Allen Mouse Brain Atlas (2nd edition) was used to identify brain regions of interest (ROIs) within the LC, DG, ACC, and AI. Two to three images were captured per region per mouse via fluorescence microscopy. Image J, an image processing software developed by the National Institutes of Health (NIH), was then used to analyze the images. Custom ROIs with unique sizes and shapes were drawn around the cell bodies of the LC, while standardized ROIs of the same size and shape were used for all ACC, AI,

and DG images. Image analysis was blinded to genotype and drug treatment, and a standard intensity threshold was set across all images for each region. Images which were obscured by bubbles or tissue tears were not used. Within the ROIs, NET fluorescent intensity and IBA-1 fluorescent intensity were quantified in Arbitrary Fluorescence Units (AFUs).

Statistical Analysis

After collecting NET and IBA-1 fluorescent intensity for each image, an average fluorescent intensity was obtained within each region for each animal. An average fluorescent intensity ± SEM was then calculated for each region in each treatment group. Separate two-way ANOVAs were used for each brain region to identify significant effects of genotype, neurotoxic injection, or the interaction of both factors. When a main effect was identified, post-hoc analyses were performed using Tukey's multiple comparison test, and differences were nonsignificant unless otherwise reported. Calculations were performed in Prism Version 8 (GraphPad Software, San Diego, CA).

Results

NET and IBA-1 fluorescent intensities were quantified in the LC, ACC, AI, and DG, and an average fluorescent intensity was obtained using three images per animal. See Figures 4, 6, 8, and 10 for the overall average ± SEM per region per group. Full results of two-way ANOVAs are presented in Table 1, and representative images are displayed in Figures 3, 5, 7, and 9. Results of post-hoc pairwise comparisons were nonsignificant unless otherwise reported.

Galanin Over-expressors

Gal OX mice in the acute paradigm were not protected against DSP-4-related degeneration

In general, the images obtained revealed no apparent differences in NET or IBA-1 fluorescent intensity in any of the brain regions after DSP-4 injection or between genotypes (Figure 3). Four separate two-way ANOVAs for the LC, ACC, AI, and DG showed no effect of DSP-4 ($p=0.396$, $p=0.0676$, $p=0.192$, $p=0.124$) or of LC-derived galanin overexpression ($p=0.290$, 0.797, 0.537, 0.472), respectively, on average NET fluorescent intensity (Figure 4). However, DSP-4-injected mice of both genotypes had a slightly lower average NET intensity than their saline-injected counterparts. Full results are presented in Table 1.

In the ACC, AI, and DG, there was also no significant effect of DSP-4 ($p=0.381$, $p=0.177$, $p=0.221$) or of LC-derived galanin overexpression ($p=0.478$, $p=0.237$, $p=0.550$) on average IBA-1 fluorescent intensity. However, DSP-4-injected mice of both genotypes had a slightly higher average IBA-1 fluorescent intensity. IBA-1 was not quantified in the LC for this group.

Gal OX mice in the chronic paradigm were not protected against DSP-4-related degeneration

Based on the acquired images, NET fluorescent intensity appeared to be reduced in the animals injected with DSP-4, but no noticeable differences were present between WT and Gal OX animals. IBA-1 fluorescent intensity appeared to be increased in both WT and Gal OX animals

injected with DSP-4: both the size and number of microglia stained appeared larger in the DG, and this was particularly true in the granule cell layer. Representational images can be found in Figure 5. In the LC, ACC, AI, and DG, a two-way ANOVA showed a main effect of DSP-4 on average NET fluorescent intensity: DSP-4-injected animals had significantly lower average NET fluorescent intensity than saline controls ($p<0.0001$, $p=0.0003$, $p<0.0001$, $p=0.0158$) (Figure 6). Post-hoc analysis revealed that WT DSP-4-injected animals had significantly lower NET than WT saline-injected animals in the LC, ACC, and AI ($p=0.0022$, $p=0.0375$, $p=0.0024$) and than Gal OX saline-injected animals in the LC, ACC, and AI ($p=0.0019$, $p=0.0299$, $p=0.0019$). However, there was no main effect of LC-derived galanin overexpression ($p=0.813$, $p=0.810$, $p=0.776$, $p=0.234$) in any of the regions.

In the ACC and AI, two-way ANOVAs revealed no effect of DSP-4 on average IBA-1 fluorescent intensity ($p=0.262$, $p=0.319$). However, in the DG, DSP-4-treated animals had significantly increased IBA-1 fluorescent intensity ($p=0.0209$). There was no effect of LC-derived galanin overexpression on IBA-1 fluorescent intensity in any of the regions ($p=0.289$, $p= 0.915$, $p=0.270$). Again, IBA-1 was not quantified in the LC for this group.

Galanin Knock-outs

$Gal^{cKO\text{-}Dbh}$ mice in the acute paradigm were slightly more vulnerable to DSP-4-related degeneration

Images obtained did not show any obvious differences in NET fluorescence between groups (Figure 7). IBA-1 expression in the LC appeared very minimal. Overall, IBA-1 expression appeared dimmest in $Gal^{cKO\text{-}Dbh}$ mice that received DSP-4 injections, especially in contrast with WT mice that received DSP-4 injections. In the LC, ACC, AI, and DG, two-way ANOVA showed no effect of DSP-4 ($p=0.831$, $p=0.388$, $p=0.450$, $p=0.227$) or lack of LC-derived galanin ($p=0.954$, $p=0.438$, $p=0.201$, $p=0.606$) on average NET fluorescent intensity. However, $Gal^{cKO\text{-}Dbh}$ mice injected with DSP-4 tended to have lower average NET fluorescent intensity than WT mice injected with DSP-4 (Figure 8).

Two-way ANOVAs showed a significant effect of DSP-4 on average IBA-1 fluorescent intensity in the DG ($p=0.019$), but not in the LC, ACC, or AI ($p=0.607$, $p=0.666$, $p=0.261$). Animals injected with DSP-4 had significantly higher average IBA-1 fluorescent intensity than animals injected with saline in the DG only. Post-hoc testing revealed that in the DG, WT DSP-4-injected animals had significantly higher IBA-1 fluorescent intensity than both WT and $Gal^{cKO\text{-}Dbh}$ saline-injected animals ($p=0.0067$, $p=0.0104$).

There was a significant effect of lacking LC-derived galanin on IBA-1 fluorescent intensity in the AI and DG ($p=0.0379$, $p=0.0228$), but not in the LC or ACC ($p=0.327$, $p=0.205$). Additionally, there was a significant effect of the interaction of genotype and DSP-4 injection on average IBA-1 fluorescent intensity in the ACC and DG ($p=0.0468$, $p=0.0028$). Post-hoc testing revealed that WT DSP-4-treated animals had significantly greater IBA-1 fluorescent intensity than $Gal^{cKO\text{-}Dbh}$ DSP-4-treated animals in the DG ($p=0.0027$) and AI ($p=0.0457$).

Gal$^{cKO\text{-}Dbh}$ mice in the chronic paradigm were not more vulnerable to DSP-4-related degeneration

In general, there appeared to be no differences in NET or IBA-1 fluorescent intensity in any of the brain regions based on DSP-4 injection or genotype (Figure 9). In the LC, ACC, AI, and DG, a two-way ANOVA showed no effect of DSP-4 ($p=0.776$, $p=0.279$, $p=0.465$, $p=0.770$) or lack of LC-derived galanin ($p= 0.809$, $p=0.379$, 0.973, 0.902) on average NET fluorescent intensity (Figure 10).

Additionally, there was no effect of DSP-4 injection ($p=0.901$, $p=0.489$, $p=0.784$, $p=0.753$) or lack of LC-derived galanin ($p=0.819$, $p=0.282$, $p=0.103$, $p=0.364$) on average IBA-1 fluorescent intensity in the LC, ACC, AI, or DG. Although not a significant difference, Gal$^{cKO\text{-}Dbh}$ mice tended to have lower average IBA-1 fluorescent intensity than WT mice in most regions.

Discussion

In general, the results above recapitulate previous data showing that DSP-4 dose-dependently damages LC neurons and projections; the 50 mg/kg dose was more toxic than the 10 mg/kg dose. Furthermore, chronic exposure led to a greater reduction in average NET fluorescent intensity than acute treatment. DSP-4-induced damage was accompanied by increased IBA-1 fluorescent intensity, indicating neuroinflammation under some conditions, particularly in the DG.

Our data do not support the prediction that galanin overexpression would protect LC neurons from damage. There was no significant difference in NET or IBA-1 between and Gal OX and WT controls injected with DSP-4. This finding is distinct from previous work done by Elliot-Hunt et al. (2004) showing that non-LC-specific galanin overexpression significantly reduced hippocampal cell death following kainic acid-induced damage. However, our findings suggest that knocking out galanin in noradrenergic neurons made them more vulnerable to DSP-4 toxicity, particularly in the acute paradigm. While the genotype differences were not significant, there was a trend for reduced NET fluorescent intensity in the DSP-4-treated $Gal^{cKO\text{-}Dbh}$ animals across all forebrain projection regions studied. This finding recapitulates previous work showing greater hippocampal cell death in galanin-knockout mice than in controls after kainic acid-induced hippocampal damage (Elliot-Hunt et al., 2004).

Intriguingly, our findings indicate that the ability of DSP-4 to induce IBA-1 expression was blunted in the $Gal^{cKO\text{-}Dbh}$ mice, suggesting that LC-derived galanin may play a key role in the activation of microglia in response to damage. Microglia have been shown to both produce galanin and have galanin receptors (Shen, Larm, and Gundlach 2003; Su et al., 2003). Additionally, it has been shown that galanin induces microglial migration via GalR2, suggesting that galanin may have a role in activating microglia to respond to pathological conditions (Ifuku et al., 2011). Therefore, it is possible that lacking galanin reduces signals to microglial to activate following damage, leading to the lower average IBA-1 fluorescent intensity we observed in some $Gal^{cKO\text{-}Dbh}$ mice.

Significantly reduced IBA-1 expression was seen across most brain regions studied in the acute $Gal^{cKO\text{-}Dbh}$ paradigm, even with galanin production occurring in microglia and other parts of the brain in addition to the LC. The less apparent trends in IBA-1 in the $Gal^{cKO\text{-}Dbh}$ chronic paradigm may be a result of the process of microglial activation. Under normal conditions, microglia at rest are narrow in shape with long, thin branches, and they serve to perform surveillant activity. Rather quickly after damage, they activate, upregulate IBA-1, and adopt a more amoeboid, rounded shape with thicker and more rigid branches. In this initial response, the M1 stage, microglia promote inflammation, increase their mobility, and proliferate. Work by Ifuku et al. (2011) has shown that galanin signaling via GalR2 in microglia increases microglial mobility in a dose-dependent manner. However, with extended time following neuronal damage, microglia change in morphology and enter the M2 stage, in which they have an anti-inflammatory role and no longer promote microglial proliferation. This shift between M1 and M2 is accompanied by morphological changes, possible changes in mobility, as well as shifts in expression of various signaling proteins. Additionally, each region of the brain has different levels and predominant morphologies in response to damage (Ito et al., 1998; Jurga, Palezcna, and Kuter, 2020; Zheng and Wong, 2019). Among chronically injected mice, it is likely that microglia entered M2 or intermediate phase between M1 and M2, potentially obscuring a trend similar to what was observed in the acute paradigm.

Limitations

NET and IBA-1 fluorescent intensity were quantified in only four brain regions, using a maximum of three images, meaning that this method may not accurately represent the levels of NET throughout the entire brain. Additionally, only one dose of DSP-4 was tested in each group (10 mg/kg in $Gal^{cKO\text{-}DBH}$ mice and 50 mg/kg in Gal OX), restricting our ability to optimize the dose based on our hypothesis. Data for IBA-1 in the LC for both Gal OX groups was also not obtained due to time constraints, although very little LC IBA-1 staining was observed in all other groups. These experiments were also generally limited by the use of immunohistochemistry, which does not allow for direct measurement of levels of proteins of interest, and by the use of fluorescent intensity to measure NET and IBA-1. Using IBA-1 fluorescent intensity as an indicator of microglial activation also limited the extent of our findings, as other stains and assays could have provided more information about microglial activity.

Furthermore, this experiment was performed in mice and may have limited applicability to humans. Many similarities exist in the human and rodent nervous system. However, neurodegenerative diseases have been modelled and cured numerous times in rodents, and these results have not translated to human disease (Franco and Cedazo-Minguez, 2014). Additionally, this model of DSP-4-induced damage to the LC does not perfectly mimic damage to the LC observed in neurodegenerative disease. While chronic injection of DSP-4 produces the LC neuron death observed in later stages of neurodegenerative diseases such as AD, the degeneration occurs through different processes. Passing through the blood-brain barrier, DSP-4 is taken up by and inhibits NET. DSP-4 then accumulates in and destroys noradrenergic

terminals via unknown mechanisms (Ross and Stenfors, 2014). However, evidence suggests that AD pathology involves the accumulation of pathogenic tau in LC neurons which eventually leads to their death. The aggregation of hyperphosphorylated tau likely contributes to loss of structural integrity, synapse retraction, local inflammation, and more (Chalermpalanupap et al., 2017). Because of this consideration and the complexities involved in naturally occurring human disease, the actions of galanin in cases of LC damage in neurodegenerative disease may differ, thereby limiting the applicability of these results.

Future Directions

This study found that DSP-4-injected $Gal^{cKO\text{-}Dbh}$ mice had reduced IBA-1 expression in certain circumstances. Further work is needed to evaluate the role of galanin in promoting microglial activation in response to damage to elucidate the neuroprotective role of galanin suggested by this study and others. The role of galanin in microglial activation should be assessed in $Gal^{cKO\text{-}Dbh}$ models in both acute and chronic lesioning paradigms. Additionally, the stage of microglial activation should be assessed through quantification of the microglial surface receptors CD16, which is upregulated in the M1 phase, and CD14, which is upregulated in the M2 phase. The CD14:CD16 ratio can be used to determine the predominant microglial phase. Additionally, levels of other pro- or anti-inflammatory agents such as IL-2 and IL-4 should be assessed in galanin-overexpressing and galanin knock-out animals to determine whether galanin acts through inducing or inhibiting inflammation and whether its role changes based on the context of acute or chronic damage. (Jurga, Paleczna, and Kuter, 2020).

Conclusion

The present study evaluated the role of the neuropeptide galanin in LC damage to elucidate its neurotrophic roles in neurodegenerative diseases such as AD and PD. The results of this study affirm that DSP-4 had its intended effects of damaging the LC and further suggest that galanin may have a role in protecting LC neurons from damage and regulating microglial activation. Further work should explore the role of galanin in microglial activity in response to damage, as this may be the route through which galanin exerts its observed neuroprotective role.

Acute Gal OX							
NET				IBA-1			
	genotype factor	neurotoxin factor	interaction		genotype factor	neurotoxin factor	interaction
LC	p=0.290, F=1.23	p=0.396, F=0.775	p=0.870, F=0.0280	ACC	p=0.478, F=0.531	p=0.381, F=0.819	p=0.699, F=0.156
ACC	p=0.797, F=0.0690	p=0.0676, F=3.98	p=0.704, F=0.151	AI	p=0.237, F=1.54	p=0.177, F=2.04	p=0.680, F=0.179
AI	p=0.537, F=0.404	p=0.192, F=1.91	p=0.543, F=0.391	DG	p=0.550, F=0.377	p=0.221, F=1.66	p=0.793, F=0.0717
DG	p=0.472, F=0.552	p=0.124, F=2.74	p=0.274, F=0.124				

Chronic Gal OX							
NET				IBA-1			
	genotype factor	neurotoxin factor	interaction		genotype factor	neurotoxin factor	interaction
LC	p=0.813, F=0.0579	p<0.0001, F=46.1	p=0.899, F=0.0168	ACC	p=0.289, F=1.21	p=0.262, F=1.36	p=0.603, F=0.283
ACC	p=0.810, F=0.0599	p=0.0003, F=21.23	p=0.951, F=0.00399	AI	p=0.915, F=0.0119	p=0.319, F=1.06	p=0.943, F=0.00530
AI	p=0.776, F=0.0841	p<0.0001, F=45.26	p=0.921, F=0.0103	DG	p=0.270, F=1.31	p=0.021, F=6.65	p=0.860, F=0.0321
DG	p=0.234, F=1.54	p=0.0158, F=7.40	p=0.853, F=0.0358				

Acute Gal$^{cKO-Dbh}$							
NET				IBA-1			
	genotype factor	neurotoxin factor	interaction		genotype factor	neurotoxin factor	interaction
LC	p=0.954, F=0.00343	p=0.823, F=0.0516	p=0.523, F=0.426	LC	p=0.327, F=1.014	p=0.607, F=0.274	p=0.110, F=2.82
ACC	p=0.438, F=0.627	p=0.388, F=0.780	p=0.494, F=0.486	ACC	p=0.205, F=1.72	p=0.666, F=0.192	p=0.0468, F=4.52
AI	p=0.201, F=1.75	p=0.450, F=0.595	p=0.628, F=0.242	AI	p=0.0379, F=4.95	p=0.261, F=1.34	p=0.0876, F=3.23
DG	p=0.606, F=0.276	p=0.227, F=1.56	p=0.514, F=0.442	DG	p=0.0228, F=6.20	p=0.0190, F=6.64	p=0.00280, F=12.0

Chronic Gal$^{cKO-DBH}$							
NET				IBA-1			
	genotype factor	neurotoxin factor	interaction		genotype factor	neurotoxin factor	interaction
LC	p=0.809 F=0.609	p=0.776, F=0.0841	p=0.808, F=0.0613	LC	p=0.819, F=0.0543	p=0.901, F=0.0160	p=0.767, p=0.0913
ACC	p=0.398, F=0.754	p=0.279, F=1.253	p=0.622, F=0.254	ACC	p=0.282, F=1.24	p=0.489, F=0.500	p=0.512, F=0.448
AI	p=0.973, F=0.00122	p=0.465, F=0.558	p=0.609, F=0.272	AI	p=0.103, F=2.96	p=0.784, F=0.0779	p=0.895, F=0.0178
DG	p=0.902, F=0.0158	p=0.770, F=0.0885	p=0.891, F=0.0195	DG	p=0.364, F=0.875	p=0.753, F=0.102	p=0.832, F=0.0464

Table 1- Two-Way ANOVA Results

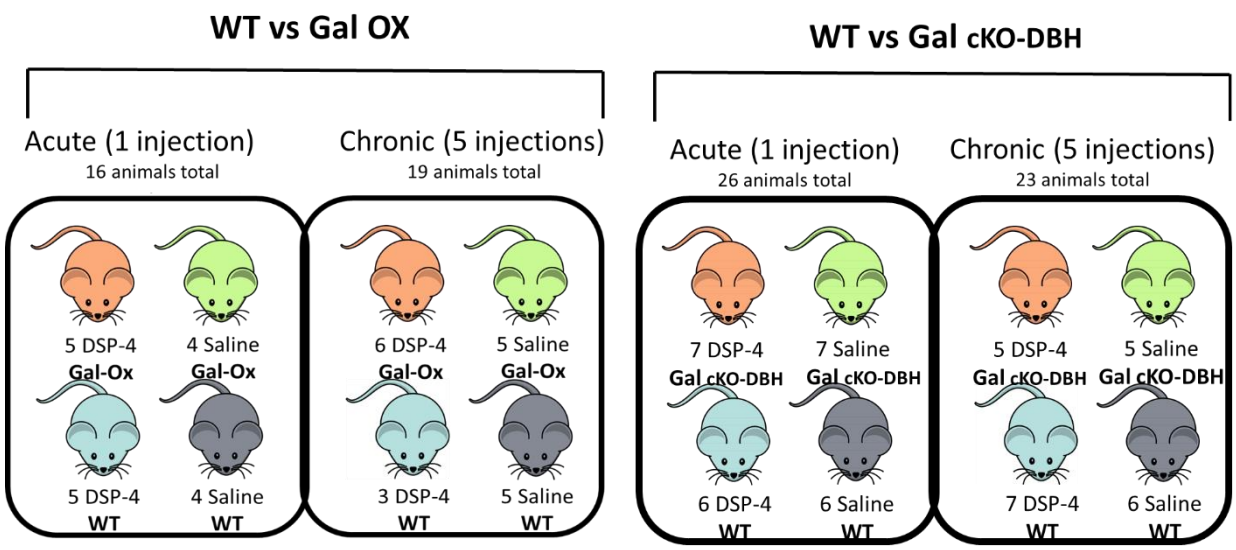

Figure 1- Experimental Design

Eighty-six mice in total were used in this study, including 20 mice overexpressing LC-derived galanin (Gal OX mice) and 24 mice with an LC-derived galanin knockout (Gal$^{cKO\text{-}Dbh}$ mice). WT saline and Gal$^{cKO\text{-}Dbh}$ or Gal OX controls were used in each group for comparison.

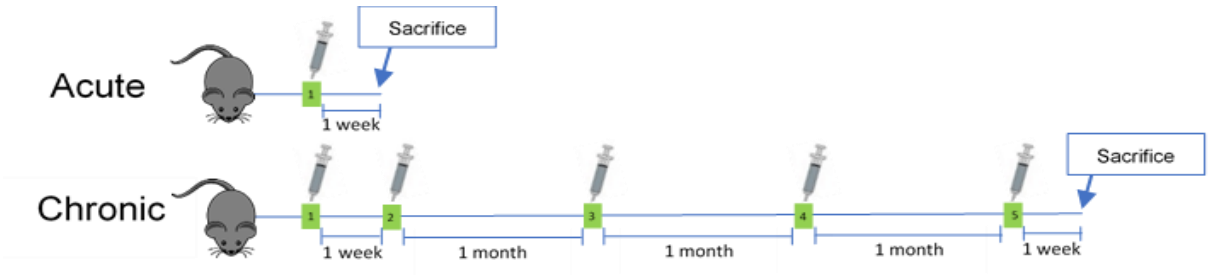

Figure 2- Injection Timeline

Animals in the acute paradigm received one injection to mimic mild LC degeneration. Animals in the chronic paradigm received a total of five injections to mimic more severe LC degeneration. One week following the last injection, all mice were sacrificed.

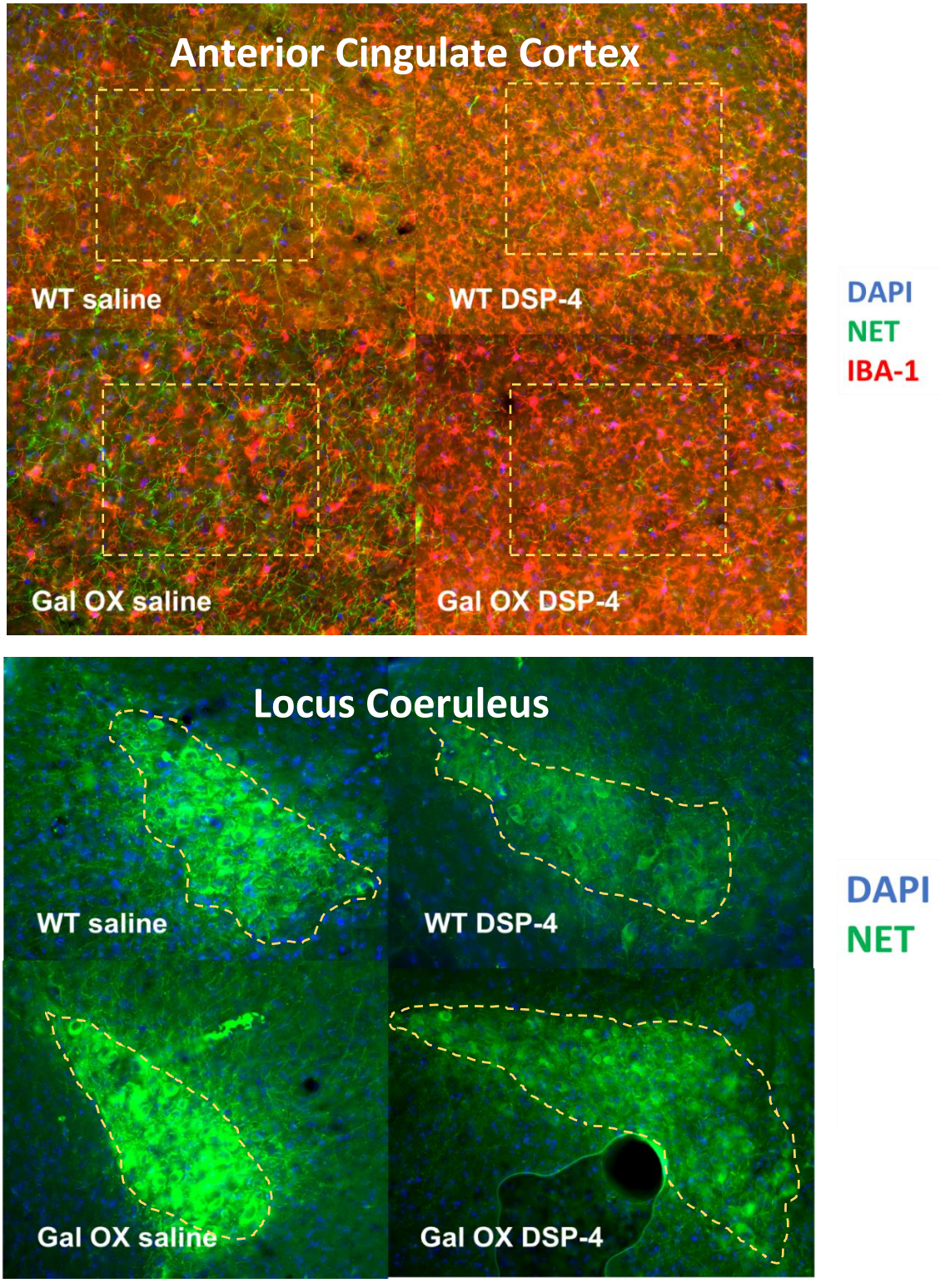

Figure 3- Acute Gal OX Representative Images. ACC (top) and LC (bottom)

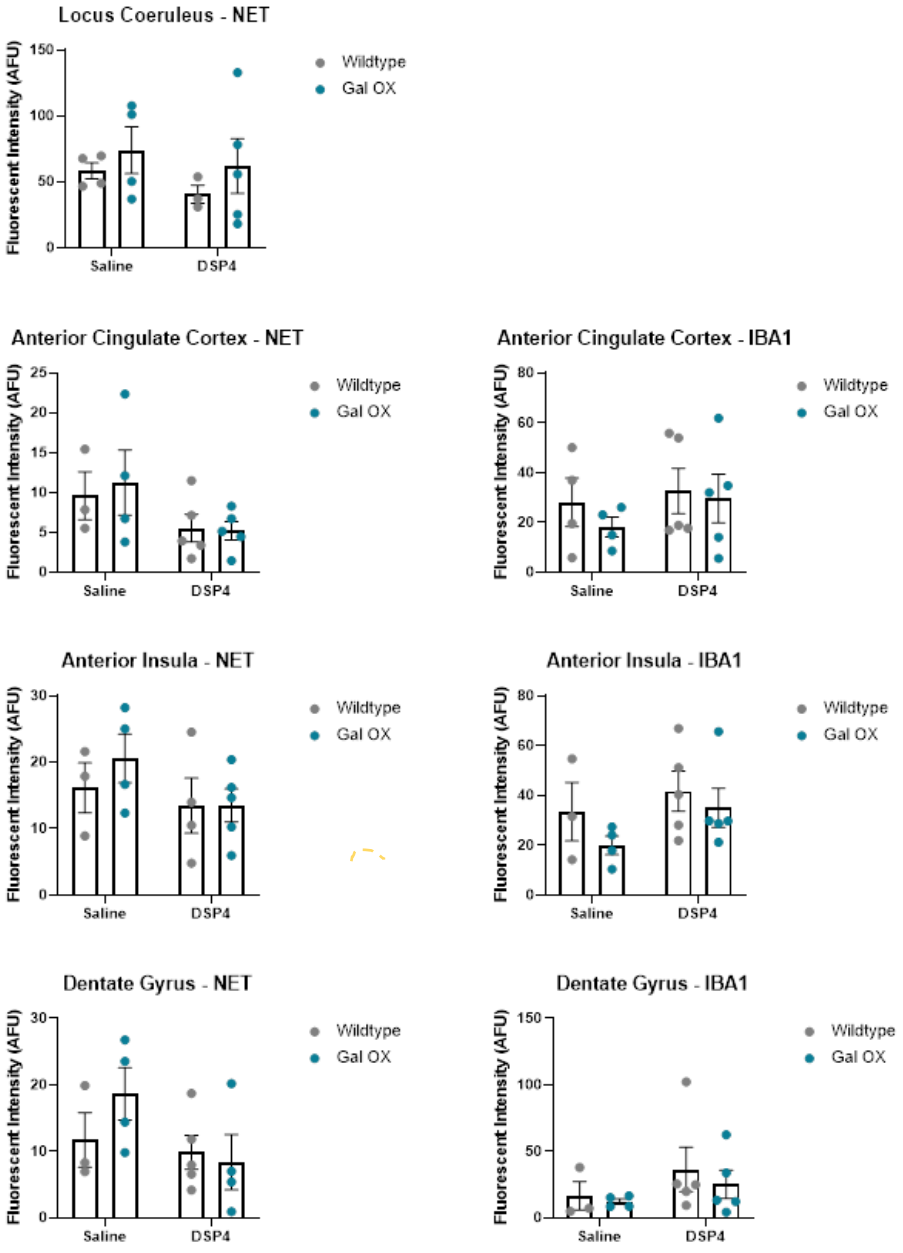

Figure 4- Acute Gal OX Results

In the LC, ACC, AI, and DG, no significant effect of DSP-4 (p=0.396, p=0.0676, p=0.192, p=0.124) or of genotype (p=0.290, 0.797, 0.537, 0.472) was identified for NET, though DSP-4-injected mice of both genotypes had a slightly lower average NET intensity than their saline-injected counterparts. In the ACC, AI, and DG, there was also no significant effect of DSP-4 (p=0.381, p=0.177, p=0.2205) or of genotype (p=0.478, p=0.237, p=0.550) on average IBA-1 fluorescent intensity. However, DSP-4-injected mice of both genotypes had a slightly higher average IBA-1 fluorescent intensity. IBA-1 was not quantified in the LC for this group.

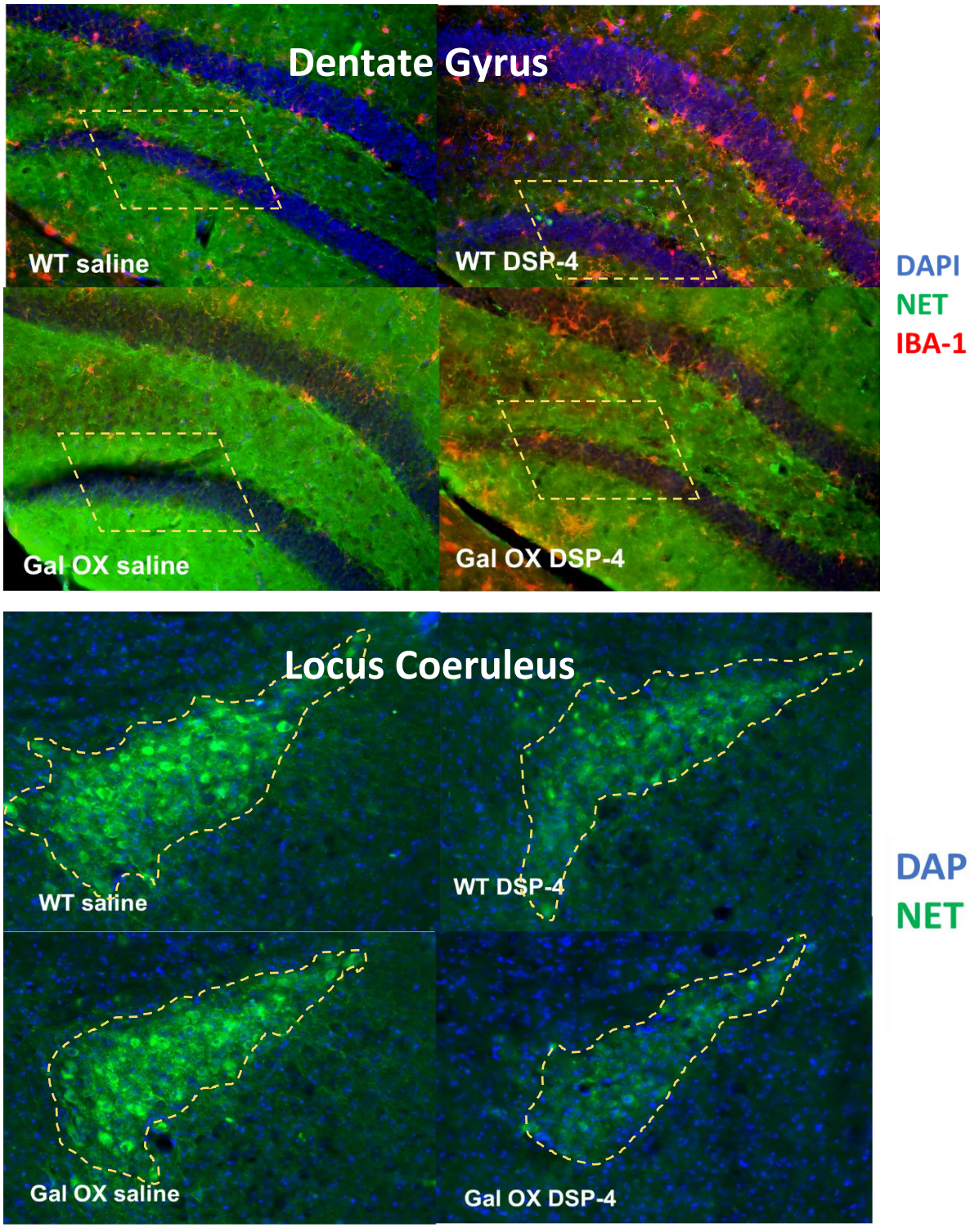

Figure 5- Chronic Gal OX Representative Images. DG (top) and LC (bottom)

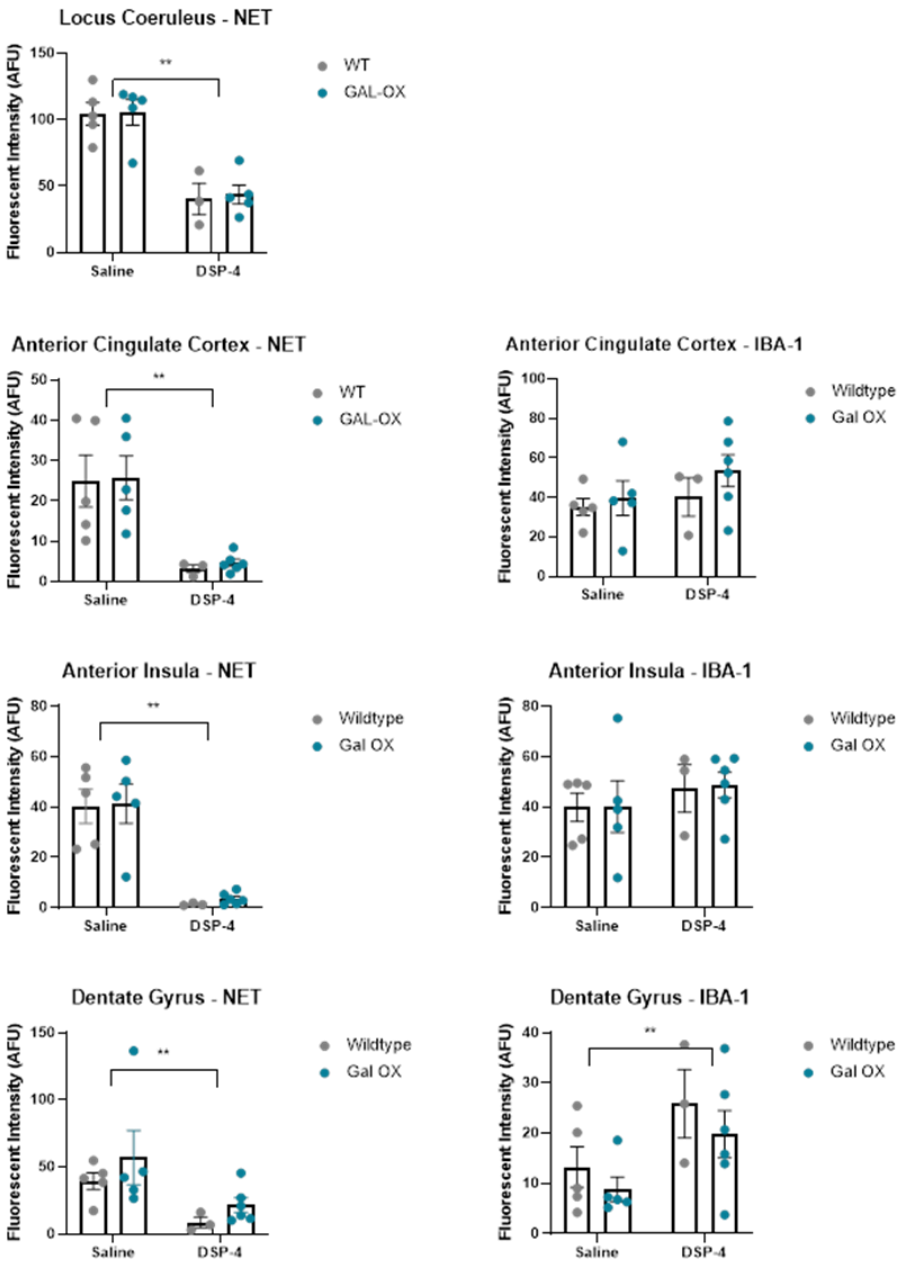

Figure 6- Chronic Gal OX Results

DSP-4-injected animals had significantly lower average NET fluorescent intensity than saline controls ($p<0.0001$, $p=0.0003$, $p<0.0001$, $p=0.0158$) (Figure 8). Post-hoc analysis revealed that WT DSP-4-injected animals had significantly lower NET than WT saline-injected animals in the LC, ACC, and AI ($p=0.0022$, $p=0.0375$, $p=0.0024$) and than Gal OX saline-injected animals in the LC, ACC, and AI ($p=0.0019$, $p=0.0299$, $p=0.0019$). However, there was no main effect of LC-derived galanin overexpression ($p=0.813$, $p=0.810$, $p=0.776$, $p=0.234$) in any of the regions.

Figure 6 (Cont'd)

In the ACC and AI, two-way ANOVAs revealed no effect of DSP-4 on average IBA-1 fluorescent intensity ($p=0.262$, $p=0.319$). However, in the DG, DSP-4-treated animals had significantly reduced IBA-1 fluorescent intensity ($p=0.0209$). There was no effect of LC-derived galanin overexpression on IBA-1 fluorescent intensity in any of the regions ($p=0.289$, $p= 0.915$, $p=0.270$). Again, IBA-1 was not quantified in the LC for this group.

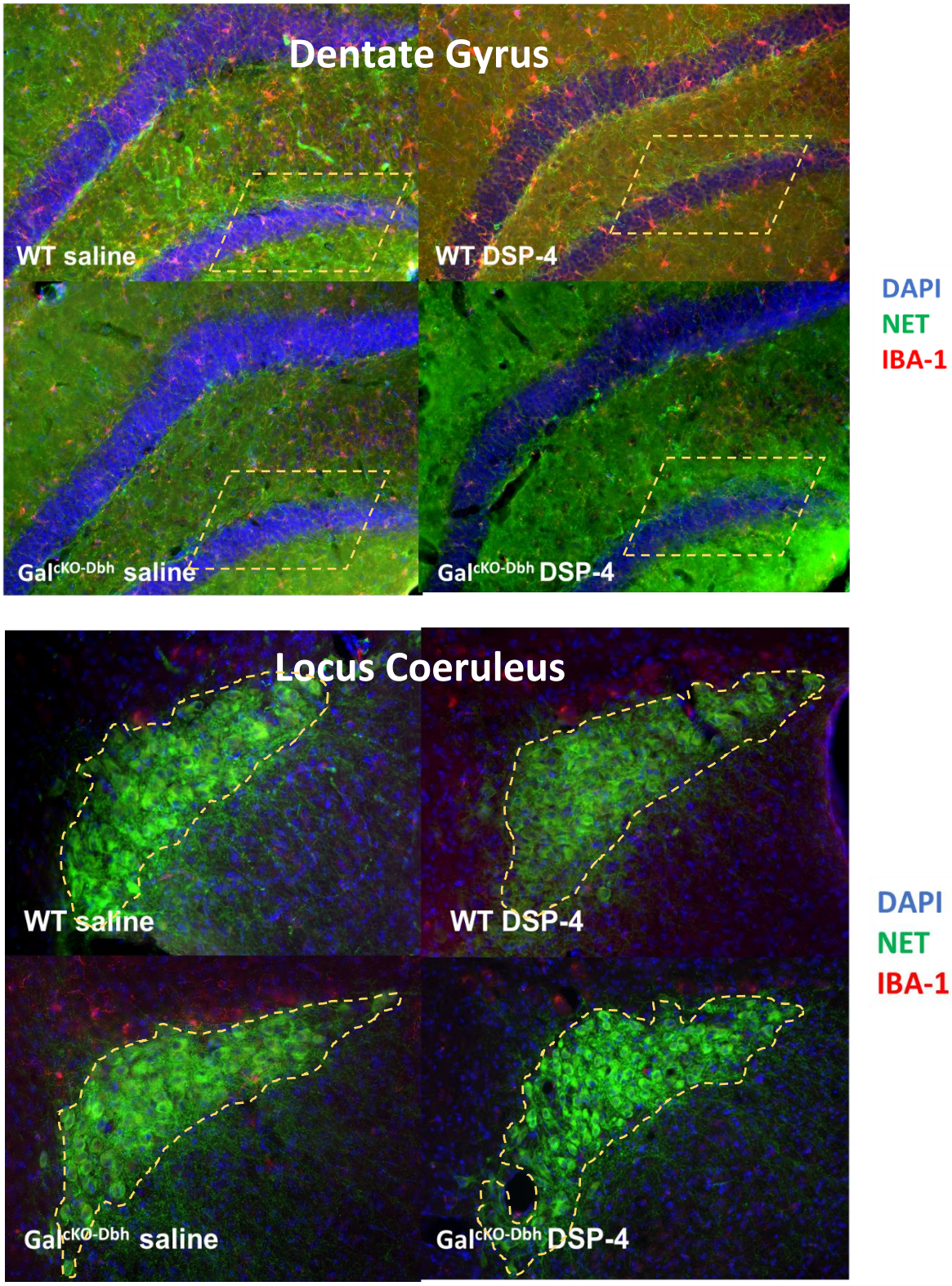

Figure 7- Acute Gal$^{cKO\text{-}Dbh}$ Representative Images. DG (top) and LC (bottom)

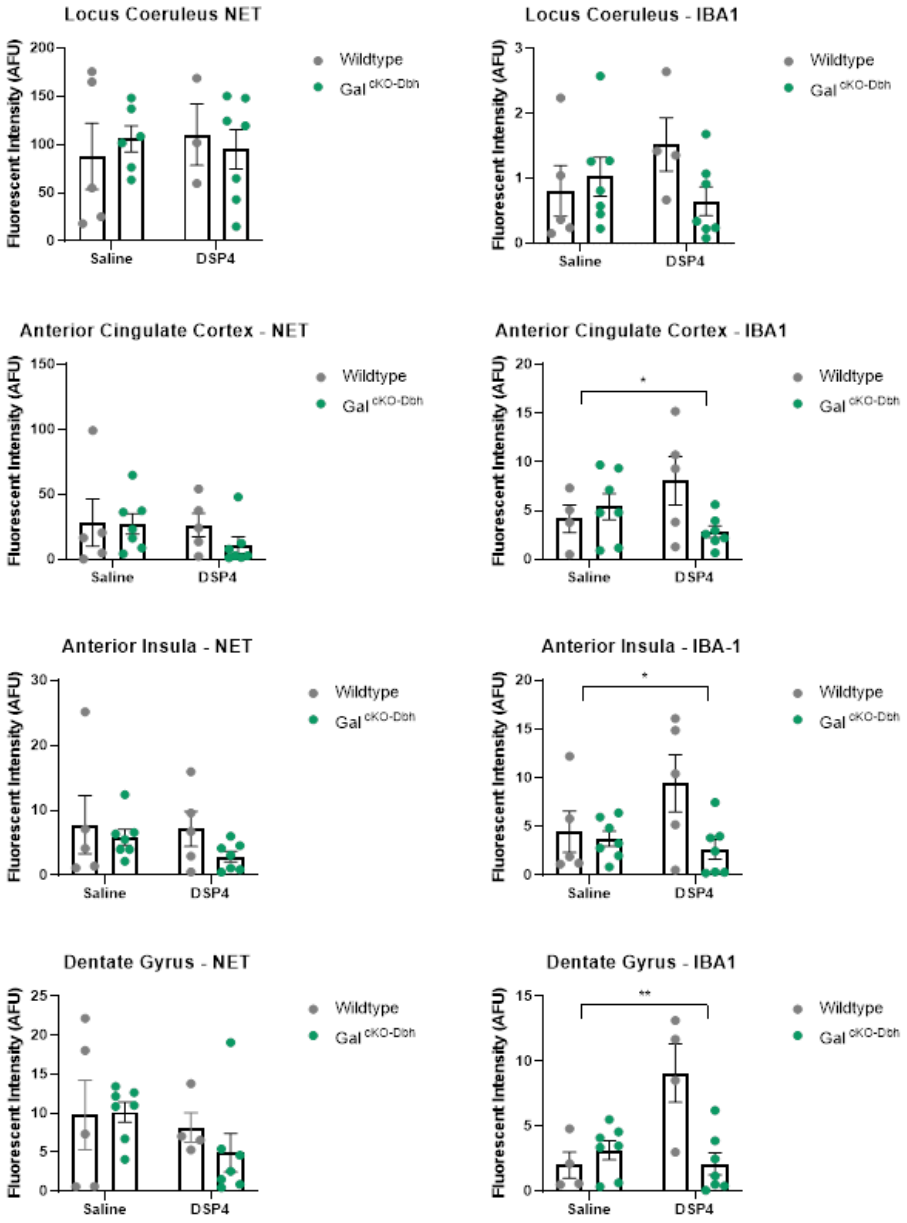

Figure 8- Acute Gal$^{cKO\text{-}Dbh}$ Results

In the LC, ACC, AI, and DG, two-way ANOVAs showed no effect of DSP-4 (p=0.831, p=0.388, p=0.450, p=0.227) or lack of LC-derived galanin (p=0.954, p=0.438, p=0.201, p=0.606) on average NET fluorescent intensity. However, Gal$^{cKO\text{-}Dbh}$ mice injected with DSP-4 tended to have lower average NET fluorescent intensity than WT mice injected with DSP-4. Two-way ANOVAs showed a significant effect of DSP-4 on average IBA-1 fluorescent intensity in the DG (p=0.019), but not in the LC, ACC, or AI (p=0.607, p=0.666, p=0.261): animals injected with DSP-4 had significantly higher average IBA-1 fluorescent intensity than animals injected with saline in the DG only.

Figure 8 (Cont'd)

Post-hoc testing revealed that in the DG, both and $Gal^{cKO\text{-}Dbh}$ saline-injected animals had significantly lower IBA-1 fluorescent intensity than WT DSP-4-injected animals (p=0.0067, p=0.0104). There was a significant effect of lacking LC-derived galanin on IBA-1 fluorescent intensity in the AI and DG (p=0.0379, p=0.0228), but not in the LC or ACC (p=0.327, p=0.205). Post-hoc testing revealed that WT DSP-4-treated animals had significantly greater IBA-1 fluorescent intensity than $Gal^{cKO\text{-}Dbh}$ DSP-4-treated animals in the DG (p=0.0027) and AI (p=0.0457). Additionally, there was a significant effect of the interaction of genotype and DSP-4 injection on average IBA-1 fluorescent intensity in the ACC, AI, and DG (p=0.0468, p=0.0379, p=0.0028); WT DSP-4-injected animals showed significantly increased IBA-1 compared to all other groups, while $Gal^{cKO\text{-}Dbh}$ DSP-4-injected animals did not exhibit this increase.

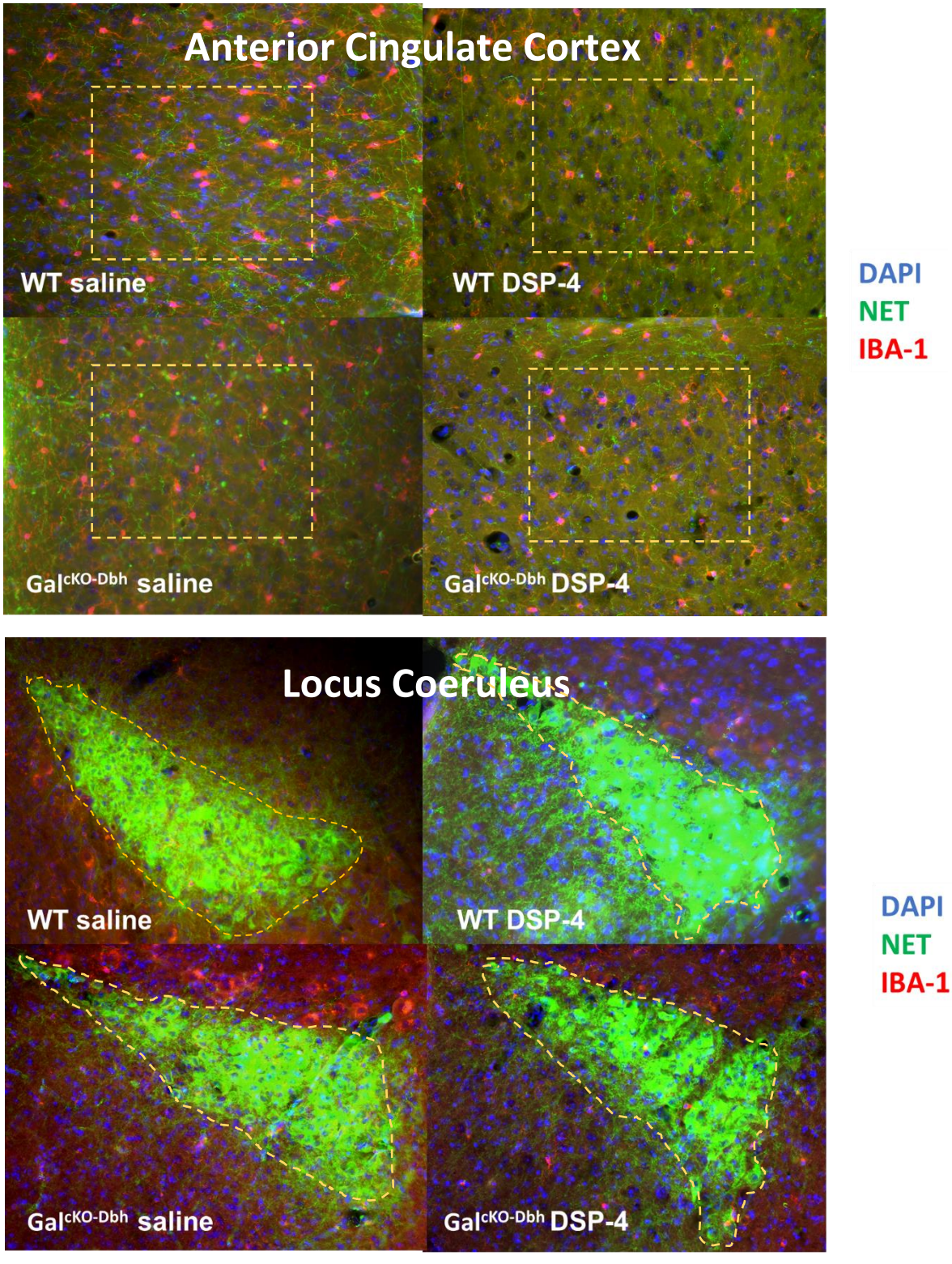

Figure 9- Chronic Gal$^{cKO\text{-}Dbh}$ Representative Images. ACC (top) and LC (bottom).

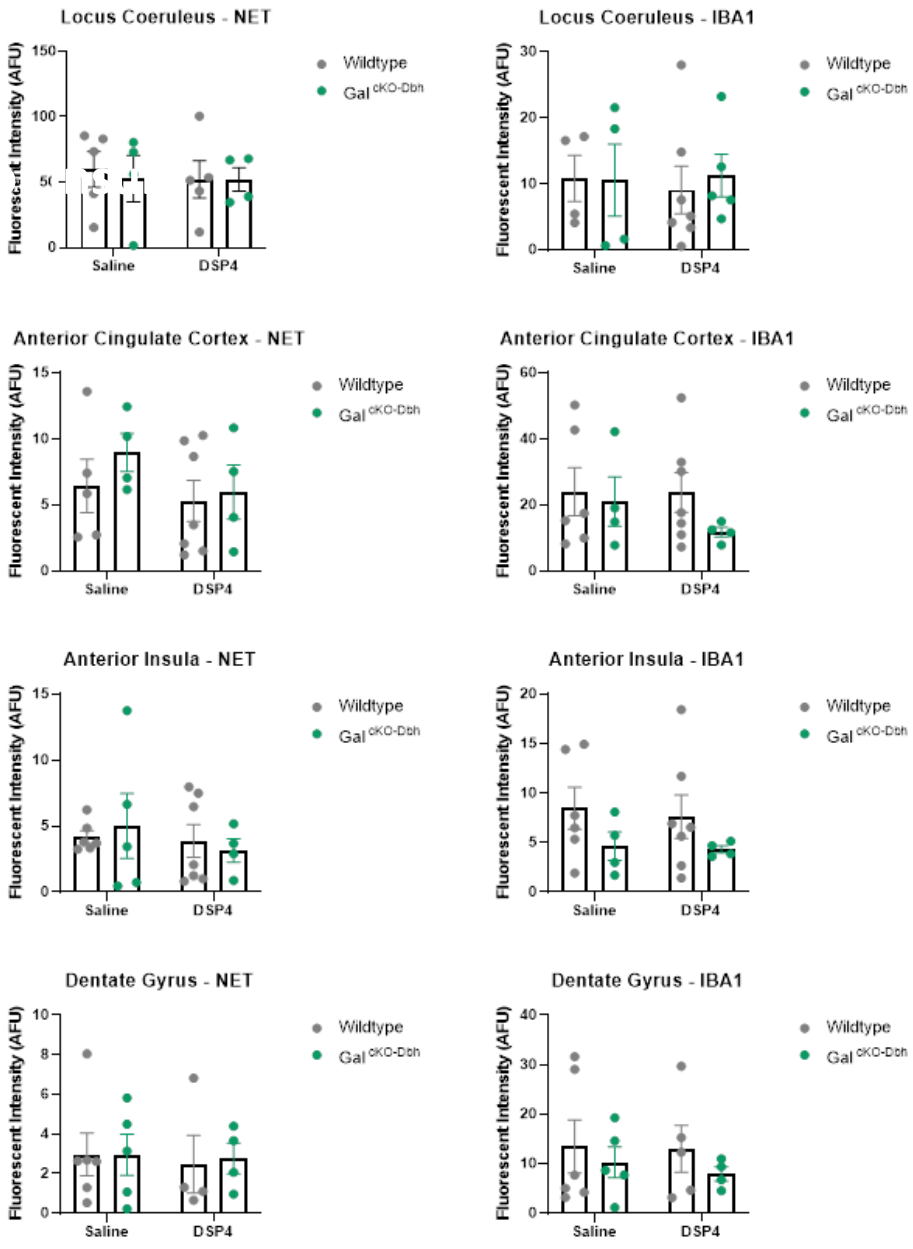

Figure 10- Chronic Gal$^{cKO\text{-}Dbh}$ Results

In the LC, ACC, AI, and DG, a two-way ANOVA showed no effect of DSP-4 (p=0.776, p=0.279, p=0.465, p=0.770) or lack of LC-derived galanin (p= 0.809, p=0.379, 0.973, 0.902) on average NET fluorescent intensity (Figure 10). Additionally, there was no effect of DSP-4 injection (p=0.901, p=0.489, p=0.784, p=0.753) or lack of LC-derived galanin (p=0.819, p=0.282, p=0.103, p=0.364) on average IBA-1 fluorescent intensity in the LC, ACC, AI, or DG. Although not a significant difference, Gal$^{cKO\text{-}Dbh}$ mice tended to have lower average IBA-1 fluorescent intensity than WT mice in most regions.

Works Cited

Aston-Jones, G., & Cohen, J. D. (2005). An integrative theory of locus coeruleus-norepinephrine function: adaptive gain and optimal performance. *Annual review of neuroscience*, *28*, 403–450. https://doi.org/10.1146/annurev.neuro.28.061604.135709

Bacon, T. J., Pickering, A. E., & Mellor, J. R. (2020). Noradrenaline Release from Locus Coeruleus Terminals in the Hippocampus Enhances Excitation-Spike Coupling in CA1 Pyramidal Neurons Via β-Adrenoceptors. *Cerebral cortex (New York, N.Y. : 1991)*, *30*(12), 6135–6151. https://doi.org/10.1093/cercor/bhaa159

Beal, M. F., MacGarvey, U., & Swartz, K. J. (1990). Galanin immunoreactivity is increased in the nucleus basalis of Meynert in Alzheimer's disease. *Annals of neurology*, *28*(2), 157–161. https://doi.org/10.1002/ana.410280207

Braak, H., & Braak, E. (1991). Neuropathological stageing of Alzheimer-related changes. *Acta neuropathologica*, *82*(4), 239–259. https://doi.org/10.1007/BF00308809

Braak, H., & Del Tredici, K. (2012). Where, when, and in what form does sporadic Alzheimer's disease begin?. *Current opinion in neurology*, *25*(6), 708–714. https://doi.org/10.1097/WCO.0b013e32835a3432

Chalermpalanupap, T., Schroeder, J. P., Rorabaugh, J. M., Liles, L. C., Lah, J. J., Levey, A. I., & Weinshenker, D. (2018). Locus Coeruleus Ablation Exacerbates Cognitive Deficits, Neuropathology, and Lethality in P301S Tau Transgenic Mice. *The Journal of neuroscience : the official journal of the Society for Neuroscience*, *38*(1), 74–92. https://doi.org/10.1523/JNEUROSCI.1483-17.2017

Chiodo, L. A., Acheson, A. L., Zigmond, M. J., & Stricker, E. M. (1983). Subtotal destruction of central noradrenergic projections increases the firing rate of locus coeruleus cells. *Brain research*, *264*(1), 123–126. https://doi.org/10.1016/0006-8993(83)91128-9

Counts, S. E., Perez, S. E., Ginsberg, S. D., De Lacalle, S., & Mufson, E. J. (2003). Galanin in Alzheimer disease. *Molecular interventions*, *3*(3), 137–156. https://doi.org/10.1124/mi.3.3.137

Counts, S. E., Perez, S. E., Ginsberg, S. D., & Mufson, E. J. (2010). Neuroprotective role for galanin in Alzheimer's disease. *Experientia supplementum (2012)*, *102*, 143–162. https://doi.org/10.1007/978-3-0346-0228-0_11

Counts, S. E., Perez, S. E., & Mufson, E. J. (2008). Galanin in Alzheimer's disease: neuroinhibitory or neuroprotective?. *Cellular and molecular life sciences : CMLS*, *65*(12), 1842–1853. https://doi.org/10.1007/s00018-008-8159-2

Crawley, J. N., Mufson, E. J., Hohmann, J. G., Teklemichael, D., Steiner, R. A., Holmberg, K., Xu, Z. Q., Blakeman, K. H., Xu, X. J., Wiesenfeld-Hallin, Z., Bartfai, T., & Hökfelt, T. (2002). Galanin overexpressing transgenic mice. *Neuropeptides*, *36*(2-3), 145–156. https://doi.org/10.1054/npep.2002.0891.

Diez, M., Koistinaho, J., Kahn, K., Games, D., & Hökfelt, T. (2000). Neuropeptides in hippocampus and cortex in transgenic mice overexpressing V717F beta-amyloid precursor protein--initial observations. *Neuroscience*, *100*(2), 259–286. https://doi.org/10.1016/s0306-4522(00)00261-x

Del Tredici, K., & Braak, H. (2013). Dysfunction of the locus coeruleus-norepinephrine system and related circuitry in Parkinson's disease-related dementia. *Journal of neurology, neurosurgery, and psychiatry*, *84*(7), 774–783. https://doi.org/10.1136/jnnp-2011-301817

Elliott-Hunt, C. R., Marsh, B., Bacon, A., Pope, R., Vanderplank, P., & Wynick, D. (2004). Galanin acts as a neuroprotective factor to the hippocampus. *Proceedings of the National Academy of Sciences of the United States of America*, *101*(14), 5105–5110. https://doi.org/10.1073/pnas.0304823101

Franco, R., & Cedazo-Minguez, A. (2014). Successful therapies for Alzheimer's disease: why so many in animal models and none in humans?. *Frontiers in pharmacology*, *5*, 146. https://doi.org/10.3389/fphar.2014.00146

Fisone, G., Wu, C. F., Consolo, S., Nordström, O., Brynne, N., Bartfai, T., Melander, T., & Hökfelt, T. (1987). Galanin inhibits acetylcholine release in the ventral hippocampus of the rat: histochemical, autoradiographic, in vivo, and in vitro studies. *Proceedings of the National Academy of Sciences of the United States of America*, *84*(20), 7339–7343. https://doi.org/10.1073/pnas.84.20.7339

Gabriel, S. M., Knott, P. J., & Haroutunian, V. (1995). Alterations in cerebral cortical galanin concentrations following neurotransmitter-specific subcortical lesions in the rat. *The Journal of neuroscience : the official journal of the Society for Neuroscience*, *15*(8), 5526–5534. https://doi.org/10.1523/JNEUROSCI.15-08-05526.1995

Grzanna, R., Berger, U., Fritschy, J. M., & Geffard, M. (1989). Acute action of DSP-4 on central norepinephrine axons: biochemical and immunohistochemical evidence for differential effects. *Journal of Histochemistry & Cytochemistry*, *37*(9), 1435–1442. https://doi.org/10.1177/37.9.2768812

Haglund, M., Sjöbeck, M., & Englund, E. (2006). Locus ceruleus degeneration is ubiquitous in Alzheimer's disease: possible implications for diagnosis and treatment. *Neuropathology : official journal of the Japanese Society of Neuropathology*, *26*(6), 528–532. https://doi.org/10.1111/j.1440-1789.2006.00725.x

Heneka, M. T., Ramanathan, M., Jacobs, A. H., Dumitrescu-Ozimek, L., Bilkei-Gorzo, A., Debeir, T., Sastre, M., Galldiks, N., Zimmer, A., Hoehn, M., Heiss, W. D., Klockgether, T., & Staufenbiel, M. (2006). Locus ceruleus degeneration promotes Alzheimer pathogenesis in amyloid precursor protein 23 transgenic mice. *The Journal of neuroscience : the official journal of the Society for Neuroscience*, *26*(5), 1343–1354. https://doi.org/10.1523/JNEUROSCI.4236-05.2006

Huang, H. P., Zhu, F. P., Chen, X. W., Xu, Z. Q., Zhang, C. X., & Zhou, Z. (2012). Physiology of quantal norepinephrine release from somatodendritic sites of neurons in locus coeruleus. *Frontiers in molecular neuroscience*, *5*, 29. https://doi.org/10.3389/fnmol.2012.00029

Ifuku, M., Okuno, Y., Yamakawa, Y., Izumi, K., Seifert, S., Kettenmann, H., & Noda, M. (2011). Functional importance of inositol-1,4,5-triphosphate-induced intracellular Ca2+ mobilization in galanin-induced microglial migration. *Journal of neurochemistry*, *117*(1), 61–70. https://doi.org/10.1111/j.1471-4159.2011.07176.x

Ito, D., Imai, Y., Ohsawa, K., Nakajima, K., Fukuuchi, Y., & Kohsaka, S. (1998). Microglia-specific localisation of a novel calcium binding protein, Iba1. *Brain research. Molecular brain research*, *57*(1), 1–9. https://doi.org/10.1016/s0169-328x(98)00040-0

Jacobowitz, D. M., Kresse, A., & Skofitsch, G. (2004). Galanin in the brain: chemoarchitectonics and brain cartography--a historical review. *Peptides*, *25*(3), 433–464. https://doi.org/10.1016/j.peptides.2004.02.015

Janitzky K. (2020). Impaired Phasic Discharge of Locus Coeruleus Neurons Based on Persistent High Tonic Discharge-A New Hypothesis With Potential Implications for Neurodegenerative Diseases. *Frontiers in neurology*, *11*, 371. https://doi.org/10.3389/fneur.2020.00371

Jardanhazi-Kurutz, D., Krummer, M.P., Terwel, D., Vogel, K., Dyrks, T., Thiele, A., Heneka, M.T. (2010) Induced LC degeneration in APP/PS1 transgenic mice accelerates early cerebral amyloidosis and cognitive deficits. *Neurochem. Int*, 57(4), 375-382. doi: 10.1016/j.neuint.2010.02.001

Jurga, A. M., Paleczna, M., & Kuter, K. Z. (2020). Overview of General and Discriminating Markers of Differential Microglia Phenotypes. *Frontiers in cellular neuroscience*, *14*, 198. https://doi.org/10.3389/fncel.2020.00198

Lang, R., Gundlach, A. L., Holmes, F. E., Hobson, S. A., Wynick, D., Hökfelt, T., & Kofler, B. (2015). Physiology, signaling, and pharmacology of galanin peptides and receptors: three

decades of emerging diversity. *Pharmacological reviews*, *67*(1), 118–175. doi: 10.1124/pr.112.006536.

Lin, H. & Vartanian, O. (2018). A Neuroeconomic Framework for Creative Cognition. *Perspectives on Psychological Science, 13*. https://doi.org/10.1177/1745691618794945

Loughlin, S. E., Foote, S. L., & Grzanna, R. (1986). Efferent projections of nucleus locus coeruleus: morphologic subpopulations have different efferent targets. *Neuroscience*, *18*(2), 307–319. https://doi.org/10.1016/0306-4522(86)90156-9

Ma, X., Tong, Y. G., Schmidt, R., Brown, W., Payza, K., Hodzic, L., Pou, C., Godbout, C., Hökfelt, T., & Xu, Z. Q. (2001). Effects of galanin receptor agonists on locus coeruleus neurons. *Brain research*, *919*(1), 169–174. doi: 10.1016/s0006-8993(01)03033-5.

Matchett, B. J., Grinberg, L. T., Theofilas, P., & Murray, M. E. (2021). The mechanistic link between selective vulnerability of the locus coeruleus and neurodegeneration in Alzheimer's disease. *Acta neuropathologica*, 141(5). 10.1007/s00401-020-02248-1. Advance online publication. doi: 10.1007/s00401-020-02248-1.

Mufson, E. J., Deecher, D. C., Basile, M., Izenwasse, S., & Mash, D. C. (2000). Galanin receptor plasticity within the nucleus basalis in early and late Alzheimer's disease: an in vitro autoradiographic analysis. *Neuropharmacology*, *39*(8), 1404–1412. https://doi.org/10.1016/s0028-3908(00)00011-3

Musacchio JM (2013). "Chapter 1: Enzymes involved in the biosynthesis and degradation of catecholamines". In Iverson L (ed.). *Biochemistry of Biogenic Amines*. Springer. pp. 1–35. ISBN 978-1-4684-3171-1.

Oertel, W. H., Henrich, M. T., Janzen, A., & Geibl, F. F. (2019). The locus coeruleus: Another vulnerability target in Parkinson's disease. *Movement disorders : official journal of the Movement Disorder Society*, *34*(10), 1423–1429. https://doi.org/10.1002/mds.27785

Oleskevich S, Descarries L, Lacaille J. (1989). Quantified distribution of the noradrenaline innervation in the hippocampus of adult rat. *J Neurosci, 9*, 3803–15. doi: 10.1523/JNEUROSCI.09-11-03803.1989

Ross, S. B., & Stenfors, C. (2015). DSP4, a selective neurotoxin for the locus coeruleus noradrenergic system. A review of its mode of action. *Neurotoxicity research*, *27*(1), 15–30. https://doi.org/10.1007/s12640-014-9482-z

Ross, S. (1976). Long-Term Effects Of N-2-Chloroethyl-N-Ethyl-2-Bromobenzylamine Hydrochloride On Noradrenergic Neurones In The Rat Brain And Heart. *British Journal of Pharmacology*, *58*(4), 521–527. doi: 10.1111/j.1476-5381.1976.tb08619.x

Samuels, E. R., & Szabadi, E. (2008). Functional neuroanatomy of the noradrenergic locus coeruleus: its roles in the regulation of arousal and autonomic function part I: principles of functional organisation. *Current neuropharmacology*, *6*(3), 235–253. https://doi.org/10.2174/157015908785777229

Sara S. J. (2009). The locus coeruleus and noradrenergic modulation of cognition. *Nature reviews. Neuroscience*, *10*(3), 211–223. https://doi.org/10.1038/nrn2573

Sara, S. J., & Bouret, S. (2012). Orienting and reorienting: the locus coeruleus mediates cognition through arousal. *Neuron*, *76*(1), 130–141. https://doi.org/10.1016/j.neuron.2012.09.011

Schwarz, L. A., & Luo, L. (2015). Organization of the locus coeruleus-norepinephrine system. *Current biology : CB*, *25*(21), R1051–R1056. https://doi.org/10.1016/j.cub.2015.09.039

Schwarz, L. A., Miyamichi, K., Gao, X. J., Beier, K. T., Weissbourd, B., DeLoach, K. E., Ren, J., Ibanes, S., Malenka, R. C., Kremer, E. J., & Luo, L. (2015). Viral-genetic tracing of the input-output organization of a central noradrenaline circuit. *Nature*, *524*(7563), 88–92. https://doi.org/10.1038/nature14600.

Shen PJ, Larm JA, Gundlach AL (2003) Expression and plasticity of galanin systems in cortical neurons, oligodendrocyte progenitors and proliferative zones in normal brain and after spreading depression. *Europ J Neurosci, 18*, 1362–1376. **https://doi.org/10.1046/j.1460-9568.2003.02860.x**

Šípková, J., Kramáriková, I., Hynie, S., & Klenerová, V. (2017). The galanin and galanin receptor subtypes, its regulatory role in the biological and pathological functions. *Physiological research*, *66*(5), 729–740. https://doi.org/10.33549/physiolres.933576

Skofitsch, G., & Jacobowitz, D. M. (1985). Immunohistochemical mapping of galanin-like neurons in the rat central nervous system. *Peptides*, *6*(3), 509–546. https://doi.org/10.1016/0196-9781(85)90118-4.

Su, Y., Ganea, D., Peng, X., & Jonakait, G. M. (2003). Galanin down-regulates microglial tumor necrosis factor-alpha production by a post-transcriptional mechanism. *Journal of neuroimmunology*, *134*(1-2), 52–60. https://doi.org/10.1016/s0165-5728(02)00397-1

Swanson, L. W., & Hartman, B. K. (1975). The central adrenergic system. An immunofluorescence study of the location of cell bodies and their efferent connections in the rat utilizing dopamine-beta-hydroxylase as a marker. *The Journal of comparative neurology*, *163*(4), 467–505. https://doi.org/10.1002/cne.901630406

Szot, P., Miguelez, C., White, S. S., Franklin, A., Sikkema, C., Wilkinson, C. W., Ugedo, L., & Raskind, M. A. (2010). A comprehensive analysis of the effect of DSP4 on the locus coeruleus noradrenergic system in the rat. *Neuroscience*, *166*(1), 279–291. https://doi.org/10.1016/j.neuroscience.2009.12.027

Szot, P., Franklin, A., Miguelez, C., Wang, Y., Vidaurrazaga, I., Ugedo, L., Sikkema, C., Wilkinson, C. W., & Raskind, M. A. (2016). Depressive-like behavior observed with a minimal loss of locus coeruleus (LC) neurons following administration of 6-hydroxydopamine is associated with electrophysiological changes and reversed with precursors of norepinephrine. *Neuropharmacology*, *101*, 76–86. https://doi.org/10.1016/j.neuropharm.2015.09.003

Tillage, R. P., Sciolino, N. R., Plummer, N. W., Lustberg, D., Liles, L. C., Hsiang, M., Powell, J. M., Smith, K. G., Jensen, P., & Weinshenker, D. (2020). Elimination of galanin synthesis in noradrenergic neurons reduces galanin in select brain areas and promotes active coping behaviors. *Brain structure & function*, *225*(2), 785–803. https://doi.org/10.1007/s00429-020-02035-4

Trillo, L., Das, D., Hsieh, W., Medina, B., Moghadam, S., Lin, B., Dang, V., Sanchez, M. M., De Miguel, Z., Ashford, J. W., & Salehi, A. (2013). Ascending monoaminergic systems alterations in Alzheimer's disease. translating basic science into clinical care. *Neuroscience and biobehavioral reviews*, *37*(8), 1363–1379. https://doi.org/10.1016/j.neubiorev.2013.05.008

Webling, K. E., Runesson, J., Bartfai, T., & Langel, U. (2012). Galanin receptors and ligands. *Frontiers in endocrinology*, *3*, 146. https://doi.org/10.3389/fendo.2012.00146

Weinshenker D. (2018). Long Road to Ruin: Noradrenergic Dysfunction in Neurodegenerative Disease. *Trends in neurosciences*, *41*(4), 211–223. https://doi.org/10.1016/j.tins.2018.01.010

Wynick, D., Thompson, S. W., & McMahon, S. B. (2001). The role of galanin as a multi-functional neuropeptide in the nervous system. *Current opinion in pharmacology*, *1*(1), 73–77. https://doi.org/10.1016/s1471-4892(01)00006-6

Zarow, C., Lyness, S. A., Mortimer, J. A., & Chui, H. C. (2003). Neuronal loss is greater in the locus coeruleus than nucleus basalis and substantia nigra in Alzheimer and Parkinson diseases. *Archives of neurology*, *60*(3), 337–341. https://doi.org/10.1001/archneur.60.3.337

Zheng, Z.V., Wong, K.C.G. (2019). Microglial activation and polarization after subarachnoid hemorrhage. *Neuroimmunol Neuroinflammation*, *6*(1). http://dx.doi.org/10.20517/2347-8659.2018.52.